

Discussion on Blasting Vibration Velocity of Deep Rock Mass Considering Thickness of Overlying Soil Layer

Jia Bin Ruan^{1*}, Tie Hang Wang¹, Zai Kun Zhao¹, Liang Zhang¹, Hong Bo Yin¹

¹ Department of Civil Engineering, College of Civil Engineering, Xi'an University of Architecture and Technology, 710055 Shaanxi, China

* Corresponding author, e-mail: ruanjiabin@xauat.edu.cn

Received: 22 May 2022, Accepted: 15 July 2023, Published online: 26 July 2023

Abstract

The thickness of the overlying soil layer has a certain influence on the blasting vibration response of deep rock mass. The vibration wave velocity of the overlying soil layer during the construction of deep blasting is measured in this paper. Based on the measured data, parameters k and α of the Sadowski equation are used to characterize the influence of the comprehensive geological conditions of the site on the vibration wave propagation. The model of blasting vibration velocity of deep rock mass is established according to the existing blasting theory, and the calculation accuracy of the model is verified according to the field blasting parameters. The new model is used to simulate different overlying soil thicknesses, and the safe allowable distance under different soil thicknesses is calculated. The calculated results show that with the increase of the thickness of the overlying soil layer, the blasting vibration velocity decreases and the attenuation velocity decreases gradually. The research results reveal the reduction effect of overlying soil thickness on blasting vibration to some extent. In the area with overlying soil layer, the safe allowable distance of blasting vibration safety can be appropriately reduced to increase the land utilization rate, which has important reference value for the blasting design and safety prediction of deep rock mass.

Keywords

deep rock blasting, vibration velocity, overlying soil layer, safe allowable distance

1 Introduction

With the rapid development of the global economy, people's demand for resources has increased dramatically, and shallow mineral resources are seriously lacking. Mineral resources are gradually moving towards deep development. According to statistics, the depth of some mines in China has exceeded 1 km [1, 2], and deep resource development will become a normal state [3]. Attention has also been paid to the impact of deep rock blasting on the construction environment, especially the blasting vibration caused by the impact of blasting seismic waves, which often has an impact on the surrounding environment [4–7]. According to China's Blasting Safety Regulations [8], blasting construction operations should be carried out outside the safe allowable distance, which is determined by blasting vibration speed and stratum conditions. With the acceleration of the modernization process, it is particularly important to improve the utilization rate of land. Determining the correct safety allowable distance is not only conducive to the safety of the surrounding

environment, but also can increase the utilization rate of land and improve the development and utilization rate of mineral resources. Therefore, it is of practical significance to study the propagation of blasting vibration velocity in deep rock mass.

During rock blasting construction, explosives release a large amount of energy to destroy rocks, and part of the energy propagates outward in the form of seismic waves, thus causing surface vibration [9, 10]. At present, a lot of research work has been carried out on blasting vibration. Crandle conducted a preliminary study on the propagation law of blasting seismic wave and the factors influencing its intensity [11]. After analyzing a large amount of data, the former Soviet Union scholar Sadowski obtained the Sadowski formula according to the similarity principle, which is widely used in blasting vibration analysis [12]. Since then, in order to modify the formula, many scholars have fitted the blasting vibration prediction formula suitable for the different sites by analyzing a large

number of field measured data [13–17]. With the progress of computer level, many scholars have studied the impact of blasting vibration on the surrounding environment based on numerical simulation and achieved good results [18–20]. In rock blasting, drilling and blasting technology is widely used because of its low cost and simple operation [21]; Yi et al. [22] analyzed the blasting process of rock under original stress from a theoretical perspective. Finite element method and discrete element method were also widely used in rock blasting [23–26]. The above analysis shows that the current research on rock blasting has achieved fruitful results. However, the existing research mainly focuses on the field of blasting vibration and mechanism research. The blasting operation of deep rock mass often encounters the condition of overlying soil layer, but there are few studies on the influence of overlying soil layer thickness on blasting vibration of rock mass.

In this paper, the regression analysis of the measured blasting vibration velocity is carried out, and the model is calculated according to the existing blasting theory and field blasting parameters. The peak value of surface blasting vibration under different soil thickness is calculated, and the safety allowable distance is calculated, respectively. It is revealed that the rock mass blasting operation in the area with overlying soil layer can appropriately reduce the safety allowable distance of blasting vibration, which plays a guiding role in similar projects.

2 Field test

2.1 Test overview

Deep blasting is adopted in return air shaft and intake air shaft of a mining area in Xianyang. The shaft depth of the return air shaft is 738.45 m, the frozen section is 674 m (including 253.09 m of surface soil section and 420.91 m of bedrock section), and the ordinary section is 64.45 m; The depth of the intake shaft is 738.45 m, and the frozen section is excavated and built at 682 m (including 253 m of surface soil and 432 m bedrock section), while the ordinary section is 56.45 m. The thickness of the overlying soil layer in this area is 253 m and the maximum explosive initiation amount in a single event is 176 kg. During on-site monitoring, blasting operations were carried out on the intake shaft, with blasting depths ranging from 456 m to 470 m. According to the geological survey of the site, it is known that the site belongs to the loess plateau landform, and the blasting site is completely covered by Quaternary loess.

The blasthole adopts the single-stage straight hole cutting method, and the charge mode is coupled charge. The hole

diameter is 45 mm, the hole depth is about 4.5 m and there are 181 blastholes. According to the construction experience and blasting design calculation, the specific blasting parameters are shown in Table 1. The charge structure adopts continuous coupling charge, and the detonation device is located at the center of the explosive.

In order to study the attenuation law of blasting vibration velocity, TC-4850 blasting vibration meter was used in this field test to detect the vibration velocity of the surface. The instrument is convenient to carry, can adapt to various complex environments, and can measure the vibration velocity in three directions in real time. In order to fully and truly reflect the surface dynamic response characteristics during blasting excavation, eight measuring points at different locations around the mine were selected for monitoring. The field test diagram is shown in Fig. 1. The field measured waveform is shown in Fig. 2.

Table 1 Blasting parameters

Name	Unit	Quantity
Borehole diameter	m	Φ 7.5
Shaft excavation section	m ²	86.546
Rock conditions	f	3~4
Priming-bomb	hair	181
Explosive	m/reel, kg/reel	0.5, 0.8

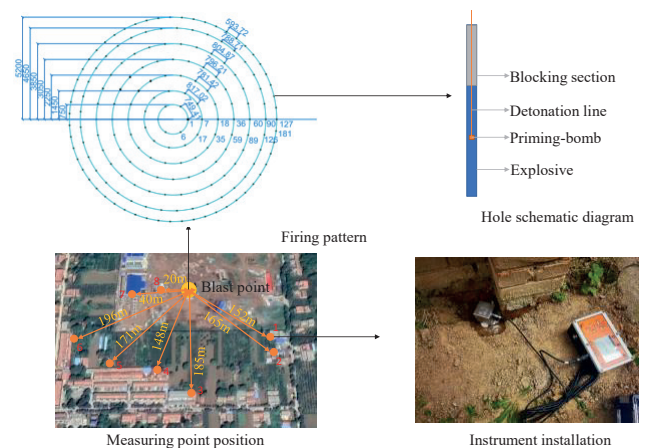


Fig. 1 Field test diagram

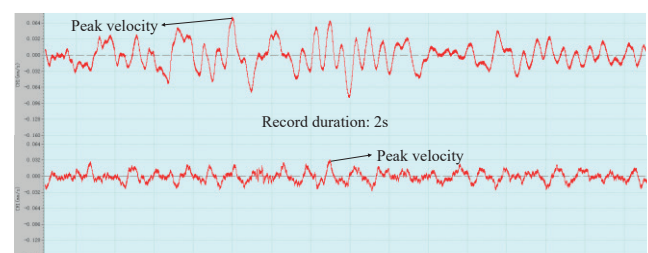


Fig. 2 Measured waveform diagram

2.2 Vibration velocity regression analysis

The vibration velocity peak in each direction measured by the measuring point of civil house foundation is shown in Table 2.

From Table 2, it can be seen that the detonation distance of measuring points 4 and 5 is the same, and the data of the two measuring points are relatively consistent indicating that the data obtained by the monitoring method in this paper are highly reliable, and the average value of the data measured by the two points is taken as the vibration velocity at this distance. The expression of Sadowski equation is as follows:

$$v = k \left(\frac{Q^{1/3}}{R} \right)^\alpha \tag{1}$$

In Eq. (1) v represents the maximum vibration velocity in the tangential, radial and vertical directions, (cm/s), and the vertical vibration velocity is taken in this paper. Q denotes the maximum amount of explosive detonation, (kg), the maximum amount of explosive blasting in this paper is 176 kg; R indicates the explosive distance, (m); k and α represent the coefficient and attenuation indexes related to topographic and geological conditions from the blasting point to the blasting monitoring point.

There is an elevation amplification effect in the propagation of blasting seismic wave, that is, the vibration velocity of the measuring point caused by blasting increases with the increase of the elevation difference between the measuring point and the blasting center. However, according to the research, the effect is only limited to a certain height difference range. When the amplification effect is not considered, the Sadowski equation can be used, which is simple in form. Only two parameters k and α are needed to characterize the influence of topography and geological conditions on vibration waves. According to the principle of least square method, linear regression analysis was conducted on x and y , where $x = 1/3 \ln Q - \ln R$, $y = \ln v$. The fitting results obtained were shown in Fig. 3.

The regression analysis shows that the linear regression coefficient r^2 is 0.912, which is greater than 0.85. The regression analysis results show that the fitting effect of the vibration velocity data in this paper is good, which can accurately reflect the vibration velocity data of the civil building foundation., and it also indicates that the civil building foundation can better reflect the propagation of blasting vibration from underground to the surface. The values of k and α can be obtained by regression analysis. According to the obtained k and α , the surface blasting

Table 2 Vibration data of measuring points

Number	Elevation (m)	Distance (m)	Velocity peak (mm/s)		
			Tangent	Radial	Vertical
1	456	480	0.035	0.071	0.085
2	456	485	0.025	0.052	0.066
3	460	483	0.029	0.068	0.079
4	460	496	0.013	0.014	0.021
5	464	496	0.012	0.014	0.022
6	464	505	0.010	0.010	0.016
7	470	472	0.066	0.079	0.108
8	470	470	0.067	0.075	0.105

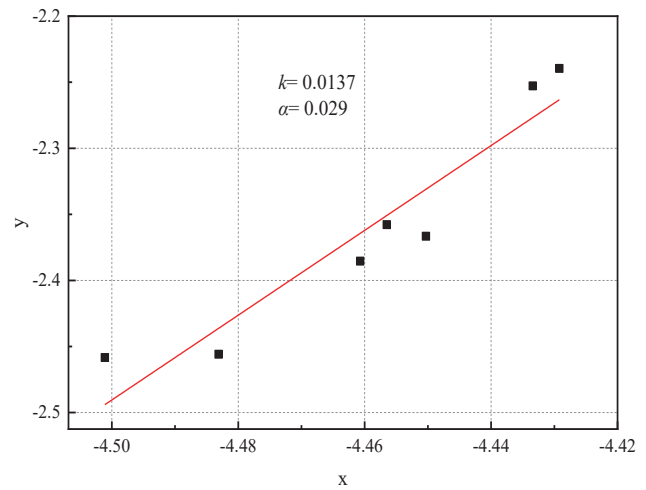


Fig. 3 Regression analysis of vibration velocity of basic measuring points

vibration velocity in this area can be predicted in the future. From the fitting results, it can be seen that under the influence of the overlying soil layer, the k and α values obtained by deep rock mass blasting are smaller. This paper further discusses through numerical simulation.

3 Numerical model

3.1 Model parameters

(1) Rock: The explosive will produce detonation waves and high temperature, high pressure detonation products in the process of explosion, which will have a strong impact and compression on the rock near the hole, making it in a state of large strain, high strain rate and high pressure.

According to this feature, the rock constitutive model uses the HJC model. The model was initially applied to concrete materials, and it has been shown that it has good applicability in the field of rock materials. It can be seen from the site geological survey that the site is basically complete and relatively complete limestone, and the relevant model parameters [27] are shown in Table 3.

Table 3 Parameters of limestone HJC constitutive model

ρ (kg/m ³)	G (MPa)	f_c (MPa)	A	B
1.72	10093	60	0.55	1.23
C	N	S_{\max}	D_1	D_2
0.0097	0.89	20	0.04	1
T (MPa)	p_c (MPa)	μ_c	μ_1	ε_0 (s ⁻¹)
4	20	0.00125	0.174	1E-6
$\varepsilon_{f,\min}$	p_1 (MPa)	K_1 (GPa)	K_2 (GPa)	K_3 (GPa)
0.01	2000	39	-223	550

In Table 3 ρ denotes the density of rock; g represents the shear modulus of rock; f_c means quasi-static uniaxial compressive strength; A , B , N and S_{\max} show the limit surface parameters, where A represents the characteristic viscous strength index, B represents the characteristic pressure hardening coefficient, N represents the pressure hardening index, and S_{\max} represents the maximum characteristic equivalent stress that the material can achieve. C represents the strain rate influence parameter; D_1 and D_2 indicate damage constants. T stands for rock tensile strength; p_c and μ_c express the net water pressure and volumetric strain of the material during crushing, respectively. p_1 and μ_1 submit the hydrostatic pressure and volumetric strain of the material during compaction, respectively. K_1 , K_2 and K_3 denote the bulk modulus of the material; ε_0 represents the reference strain rate of the material; $\varepsilon_{f,\min}$ represents the minimum plastic strain of rock fracture.

(2) Explosives: According to the blasting parameters provided in the table, the high-performance explosive materials are selected. The volume, pressure and energy characteristics of the explosive products during the blasting process are described by the JWL equation of state [28]. The JWL equation of state is expressed as:

$$P = A\left(1 - \frac{\omega}{R_1 V}\right)e^{-R_1 V} + B\left(1 - \frac{\omega}{R_2 V}\right) + \frac{\omega E_0}{V} \quad (2)$$

In Eq. (2) P represents the pressure of detonation products; E_0 denotes the initial internal energy density; V stands for the relative volume of detonation products, A and B indicate the material parameters of the explosive; R_1 , R_2 and ω represent JWL equation of state parameters. 2# emulsion explosive is selected for this model. The parameters are: density, $\rho = 1.31$ kg/m³, detonation velocity $D = 5500$ m/s, $A = 214.4$ GPa, $B = 0.182$ GPa, $R_1 = 4.2$, $R_2 = 0.9$, $\omega = 0.152$, $E_0 = 4190$ MJ/m³, $V = 1.0$.

(3) Air: Air is a model material of empty matter, and its equation of state is mostly expressed by linear polynomials. For ideal gas, it can be expressed as [29]:

$$P = C_0 + C_1 V + C_2 V^2 + C_3 V^3 + (C_4 + C_5 + C_6) \cdot \quad (3)$$

In Eq. (3) $C_0 \sim C_6$ represent the relevant parameters of the equation, where, $C_4 = C_5 = 0.4$. E_0 denotes internal energy density, $E_0 = 2500$ MJ/m³. V represents the relative volume of air, $V = 1.0$, and all remaining parameters are 0.

(4) Soil: Due to the complex variation law of soil, the elastic-plastic model based on D-P criterion is adopted, and the three-phase medium is equivalent to continuous porous medium by REV element to simplify the problem. According to the geological survey report, layered soil. The density and modulus parameters of the soil model used in this simulation were obtained by triaxial compression test and indoor compaction test. At the same time, the yield characteristics of soil under static or quasi-dynamic conditions are very different from those under blasting dynamic load. It is difficult to obtain the dynamic yield constant of soil under dynamic load through the existing test equipment and experimental methods. Therefore, this paper follows the model parameters in references [30, 31] to calculate, and the specific material parameters are shown in Table 4.

3.2 Model establishment and correctness verification

According to the blasting parameters provided in Table 1, the existing blasting theory and the above model parameters, a three-dimensional model was first established in

Table 4 Soil material parameters

Stratum code	Soil material parameters		
Q ₄	Density (kg/m ³) 1.65		
	Shear modulus (MPa) 21.5		
	Poisson ratio 0.37		
	Bulk modulus (MPa) 64.1		
Q ₃	Density (kg/m ³) 1.68		
	Shear modulus (MPa) 22.2		
	Poisson ratio 0.34		
	Bulk modulus (MPa) 63.9		
Q ₂	Density (kg/m ³) 1.76		
	Shear modulus (MPa) 22.5		
	Poisson ratio 0.34		
	Bulk modulus (MPa) 63.5		
Q ₁	Density (kg/m ³) 1.73		
	Shear modulus (MPa) 23.6		
	Poisson ratio 0.41		
	Bulk modulus (MPa) 63.7		
α_0 (Pa ²)	α_1 (Pa)	α_2	Dimensionless number
0.034	0.0007	0.3	1.5

ANSYS for trial calculation, and the model units are all SOLID164 units. Then the LS-DYNA solver is used to display the solution. According to the blasting construction parameters, the site blasting conditions are simulated. According to the layout of the blasting monitoring points, the geometric size of the model is 520 m × 340 m × 510 m. The model is divided into units to simplify the calculation process of the model, the same material is used to fill the hole blockage section and rock, and the non-reflective boundary conditions are set outside the model and on the upper and lower bottom surfaces to simulate the finite field rock medium. The whole simultaneous detonation is set as the explosive detonation mode. At the same time, due to the large size of the model, the system adopts the cm-g-μs unit system, and the time step is set to 10 μs. The schematic diagram of the model is shown in Fig. 4. The comparison between field test results and simulation results is shown in Fig. 5.

The reliability of the model is verified by simulating the three blasting conditions. The peak vibration velocity is taken, and the finite element simulation results are compared with the field measured results. The comparison

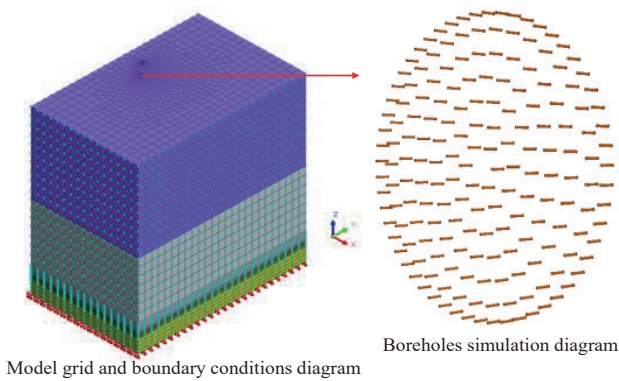


Fig. 4 Model diagram

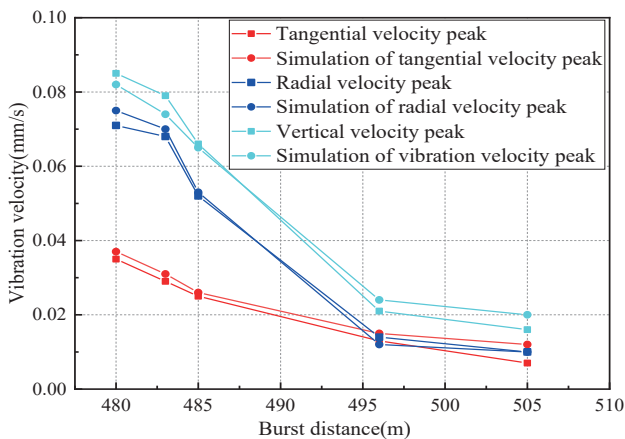


Fig. 5 Comparison of the experimental results with the simulation results

diagram is shown in the Fig. 5. The experimental results are basically consistent with the simulation results. At the same time, the values of k and α calculated by regression analysis of simulation results are $k = 0.0145$ and $\alpha = 0.0027$, respectively. The results of simulation regression analysis are not much different from those of field test regression analysis, so the model is basically accurate.

4 The influence of overlying soil thickness

In order to analyze the influence of different overlying soil thickness on the surface blasting vibration velocity, the working condition with the elevation difference of 456 m from the detonation core is calculated. Seven measuring points (1, 2, 3, 4, 6, 7 and 8) are selected as the research objects. Seven examples of overlying soil layers with thickness of 0 m, 50 m, 100 m, 150 m, 200 m, 250 m and 300 m were taken for simulation calculation. The parameters are consistent with the above simulation, and the calculated results are shown in Fig. 6.

From Fig. 6, it can be seen that with the increase of the thickness of the overlying soil layer, the vertical, radial and tangential vibration velocity peaks of each measuring point on the surface gradually decrease. At the same time, with the increase of the thickness of the soil layer, the attenuation rate of the vibration velocity peak of each measuring point becomes slower and slower, and the attenuation trend is roughly similar.

When blasting occurs in the rock layer, the gas pressure generated is very large, and it will exert a very violent compression disturbance on the surrounding medium, resulting in the high-frequency shock waves spreading around. The impact force of the shock waves is much greater than the strength of the rock, and the rock around the explosive is quickly crushed by the shock waves to form a crushing zone. The shock waves are consumed a lot of energy in the crushing zone, and the frequency is attenuated to stress waves at the edge of the crushing zone. The circumferential tensile stress caused by the stress waves causes radial cracks in the rock outside the crushing zone. At the same time, the detonation gas penetrates into the crack to further expand. With the formation of the crushing zone and radial cracks, the strain energy accumulated in the rock layer by impact compression is rapidly released to produce circumferential cracks. Under the combined action of radial and circumferential cracks, the rock layer is divided into fragments of different sizes, that is, a broken zone is formed. The area outside the fracture zone is collectively referred to as the elastic vibration zone. The stress waves and

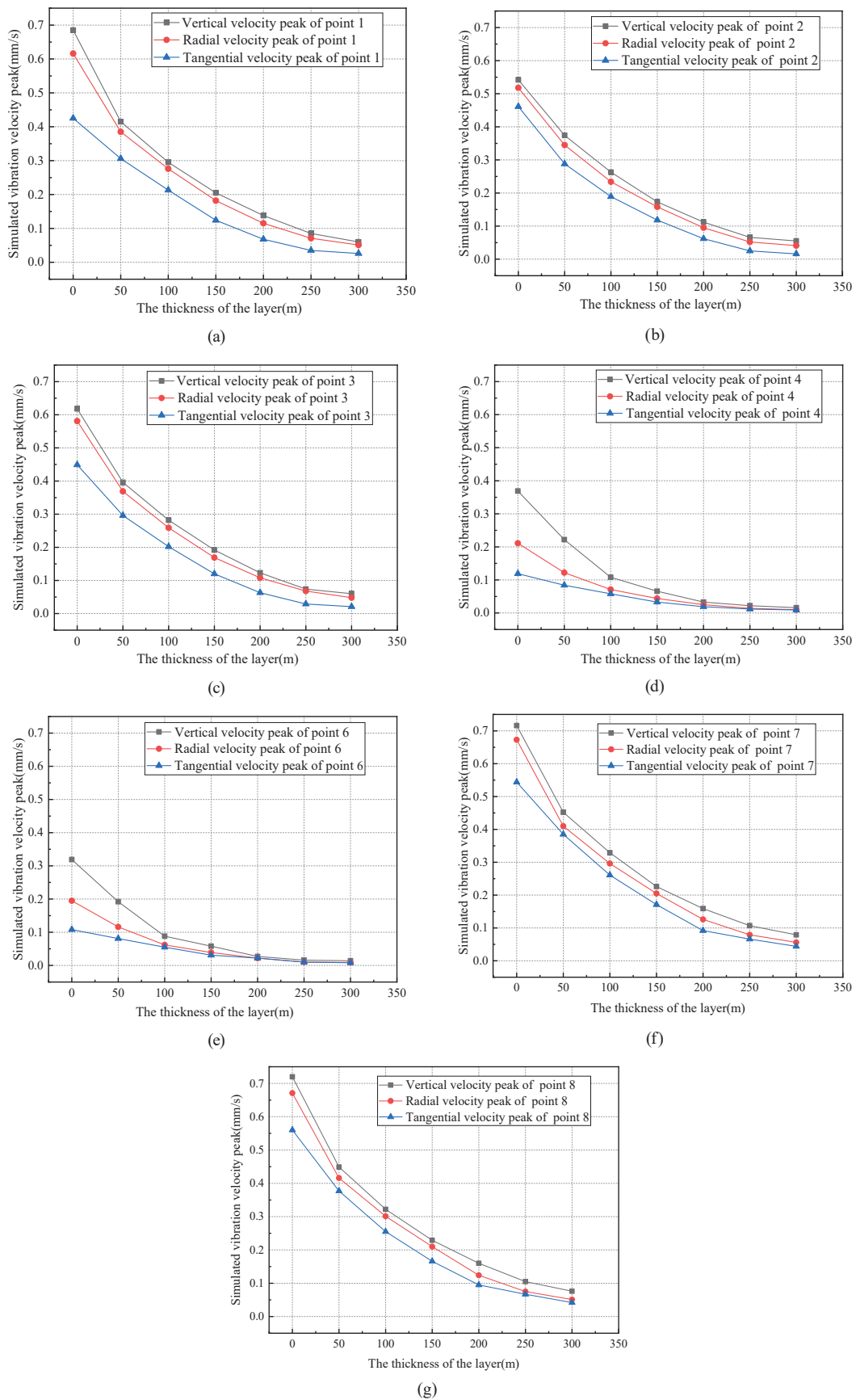


Fig. 6 Peak value of simulated vibration velocity at different soil thickness; (a) 1 measuring point, (b) 2 measuring point, (c) 3 measuring point, (d) 4 measuring point, (e) 6 measuring point, (f) 7 measuring point, (g) 8 measuring point

detonation gas in this area no longer cause rock cracking and damage, only elastic deformation occurs, and only the propagation of the low-frequency blasting seismic waves exist. The blasting seismic waves are mainly surface waves and body waves. In the elastic vibration zone, the dominant blasting seismic wave is surface wave. The surface wave is divergent, which mainly propagates along the free surface, and its propagation intensity attenuates by $R^{-1/2}$. (R is the distance from the explosion center). When it diffuses into the soil, with the increase of the blasting center distance, the blasting seismic wave continues to diffuse. Because the soil is loose material and the tensile performance is poor, radial cracks will be generated during the propagation of seismic waves, and the generation of cracks will form a failure zone. Due to its isolation effect, the transmission of stress waves will be weakened. Outside the failure zone, there is friction between soil particles, and relative displacement between soil particles will occur under the influence of seismic waves, which further dissipates the energy of seismic waves. As the thickness of the soil layer increases, the peak value of the blasting vibration velocity gradually decreases. At the same time, as the vibration velocity decreases, the attenuation rate becomes slower and slower. The schematic diagram is shown in Fig. 7.

In order to further study the influence of the thickness of the overlying soil layer on the surface blasting vibration velocity, the regression analysis of the peak vibration velocity under different thickness of the overlying soil layer is carried out, and the simulation results are brought into Eq. (1). The calculation formula of the safe allowable distance of blasting vibration [7] is:

$$R = \left(\frac{k}{v}\right)^{1/\alpha} Q^{1/3} \tag{4}$$

In Eq. (4) v is the safe allowable vibration velocity of particle where the monitoring object is located, cm/s; for civil buildings, take 1.5 cm/s. R is the safe allowable distance of blasting vibration, m. The safe allowable distance of blasting vibration is obtained by substituting k and α calculated by different soil thickness into Eq. (4). The settlement results are shown in Fig. 8.

It can be seen from Fig. 8 that when the thickness of the overlying soil layer changes from 0 m to 300 m, the safe allowable distance of blasting vibration is getting smaller and smaller. There may be errors in the numerical simulation results, but the laws revealed are somewhat illustrative. When the deep blasting operation is carried out in the

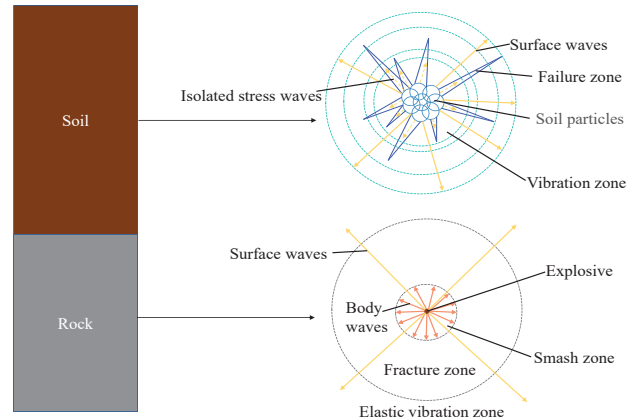


Fig. 7 Seismic wave propagation diagram

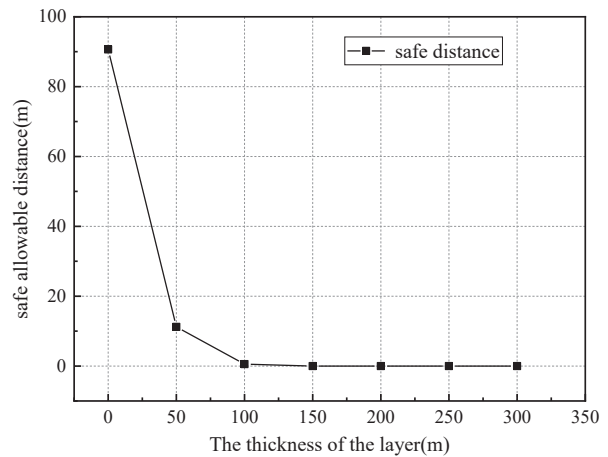


Fig. 8 Safety allowable distance under different soil thickness

area with overlying soil layer, the safe allowable distance of blasting vibration can be appropriately reduced to increase the utilization rate of land. The attenuation law of blasting vibration in soil layer and rock mass needs further study.

5 Conclusions

In this paper, through the regression analysis of the measured peak vibration velocity and the simulation of the field conditions, the thickness of different soil layers is selected for simulation calculation and regression analysis. The following main conclusions are drawn:

1. Regression analysis of measured data is carried out by Sadowski formula. Under the influence of overlying soil layer, the values of k and α are small, and the blasting vibration velocity in this area can be predicted by the fitting formula.
2. The numerical model of deep rock mass blasting is established based on the existing blasting theory. Calculation is in good agreement with the field measured data, and the reliability of the model is high.

3. The thickness of the overlying soil layer is 0 m, 50 m, 100 m, 150 m, 200 m, 250 m and 300 m, respectively. The calculation results show that with the increase of the thickness of the overlying soil layer, the peak value of the vibration velocity in each direction of the surface measuring point decreases gradually. With the increase of soil thickness, the attenuation of surface peak velocity becomes slower and slower.
4. By calculating the allowable safety distance of blasting vibration with the thickness of overlying soil layer of 0 m, 50 m, 100 m, 150 m, 200 m, 250 m and 300 m, the safe allowable distance of blasting can

be appropriately reduced in the area with overlying soil layer to increase the utilization rate of land. The attenuation law of blasting vibration in soil layer and rock needs further study. The research results have important reference value for blasting design and safety prediction of deep rock mass.

Acknowledgement

The project presented in this article is supported by the Key Science and Technology Program of Shaanxi Province (Program No. 2020ZJ-49).

References

- [1] Fan, Y., Cui, X., Leng, Z., Zheng, J., Wang, F., Xu, X. "Rockburst prediction from the perspective of energy release: A case study of a diversion tunnel at Jinping II hydropower station", *Frontiers in Earth Science*, 9, 711706, 2021.
<https://doi.org/10.3389/feart.2021.711706>
- [2] Xie, H., Konietzky, H., Zhou, H. W. "Special issue "deep mining", *Rock Mechanics and Rock Engineering*, 52(5), pp. 1415–1416, 2019.
<https://doi.org/10.1007/s00603-019-01805-9>
- [3] Ma, K., Liu, G. "Three-dimensional discontinuous deformation analysis of failure mechanisms and movement characteristics of slope rockfalls", *Rock Mechanics and Rock Engineering*, 55(1), pp. 275–296, 2022.
<https://doi.org/10.1007/s00603-021-02656-z>
- [4] Gou, Y., Shi, X., Qiu, X., Zhou, J., Chen, H., Huo, X. "Propagation characteristics of blast-induced vibration in parallel jointed rock mass", *International Journal of Geomechanics*, 19(5), 04019025, 2020.
[https://doi.org/10.1061/\(ASCE\)GM.1943-5622.0001393](https://doi.org/10.1061/(ASCE)GM.1943-5622.0001393)
- [5] Sheykhi, H., Bagherpour, R., Ghasemi, E., Kalhori, H. "Forecasting ground vibration due to rock blasting: a hybrid intelligent approach using support vector regression and fuzzy C-means clustering", *Engineering with Computers*, 34(2), pp. 357–365, 2018.
<https://doi.org/10.1007/s00366-017-0546-6>
- [6] Chen, F., He, G., Dong S., Zhao, S., Shi, L., ..., Zhang, J. "Space-time effect prediction of blasting vibration based on intelligent automatic blasting vibration monitoring system", *Applied Sciences*, 12(1), 12, 2022.
<https://doi.org/10.3390/app12010012>
- [7] General Administration of quality Supervision, China national standardization management committee, "Safety Regulations for blasting", China Communications Publishing House, Beijing, China, 2014.
- [8] Hudaverdi, T., Akyildiz, O. "Evaluation of capability of blast-induced ground vibration predictors considering measurement distance and different error measures", *Environmental Earth Sciences*, 78(14), 421, 2019.
<https://doi.org/10.1007/s12665-019-8427-5>
- [9] Lawal, A. I., Olajuyi, S. I., Kwon, S., Aladejare, A. E., Edo, T. M. "Prediction of blast-induced ground vibration using GPR and blast-design parameters optimization based on novel grey-wolf optimization algorithm", *Acta Geophysica*, 69(4), pp. 1313–1324, 2021.
<https://doi.org/10.1007/s11600-021-00607-4>
- [10] Anas, S. M., Alam, M., Umair, M. "Air-blast and ground shock-wave parameters, shallow underground blasting, on the ground and buried shallow underground blast-resistant shelters: a review", *International Journal of Protective Structures*, 13(1), pp. 99–139, 2022.
<https://doi.org/10.1177/20414196211048910>
- [11] Shi, J.-J., Guo, S.-C., Zhang, W. "Expansion of blast vibration attenuation equations for deeply buried small clearances tunnels based on dimensional analysis", *Frontiers in Earth Science*, 10, 889504, 2022.
<https://doi.org/10.3389/feart.2022.889504>
- [12] Kumar, R., Choudhury, D., Bhargava, K. "Determination of blast-induced ground vibration equations for rocks using mechanical and geological properties", *Journal of Rock Mechanics and Geotechnical Engineering*, 8(3), pp. 341–349, 2016.
<https://doi.org/10.1016/j.jrmge.2015.10.009>
- [13] Kahriman, A. "Analysis of ground vibrations caused by bench blasting at can open-pit lignite mine in Turkey", *Environmental Geology*, 41, pp. 653–661, 2002.
<https://doi.org/10.1007/s00254-001-0446-2>
- [14] Singh, P. K., Roy, M. P. "Damage to surface structures due to underground coal mine blasting: apprehension or real cause?", *Environmental Geology*, 53(6), pp. 1201–1211, 2008.
<https://doi.org/10.1007/s00254-007-0709-7>
- [15] Dindarloo, S. R. "Prediction of blast-induced ground vibrations via genetic programming", *International Journal of Mining Science and Technology*, 25(6), pp. 1011–1015, 2015.
<https://doi.org/10.1016/j.ijmst.2015.09.020>
- [16] Cardu, M., Coragliotto, D., Oreste, P. "Analysis of predictor equations for determining the blast-induced vibration in rock blasting", *International Journal of Mining Science and Technology* 29(6), pp. 905–915, 2019.
<https://doi.org/10.1016/j.ijmst.2019.02.009>

- [17] Aladejare, A. E., Lawal, A. I., Onifade, M. "Predicting the peak particle velocity from rock blasting operations using Bayesian approach", *Acta Geophysica*, 70(2), pp. 581–591, 2022.
<https://doi.org/10.1007/s11600-022-00727-5>
- [18] Blair, D. P. "Approximate models of blast vibration in non-isotropic rock masses", *International Journal of Rock Mechanics and Mining Sciences*, 128, 104245, 2020.
<https://doi.org/10.1016/j.ijrmms.2020.104245>
- [19] Duan, B., Xia, H., Yang, X. "Impacts of bench blasting vibration on the stability of the surrounding rock masses of roadways", *Tunnelling and Underground Space Technology*, 71, pp. 605–622, 2018.
<https://doi.org/10.1016/j.tust.2017.10.012>
- [20] Nateghi, R. "Prediction of ground vibration level induced by blasting at different rock units", *International Journal of Rock Mechanics and Mining Sciences*, 48(6), pp. 899–908, 2011.
<https://doi.org/10.1016/j.ijrmms.2011.04.014>
- [21] Wan, D., Zhu, Z., Liu, R., Liu, B., Li, J. "Measuring method of dynamic fracture toughness of mode I crack under blasting using a rectangle specimen with a crack and edge notches", *International Journal of Rock Mechanics and Mining Sciences*, 123, 104104, 2019.
<https://doi.org/10.1016/j.ijrmms.2019.104104>
- [22] Yi, C., Johansson, D., Greberg, J. "Effects of in-situ stresses on the fracturing of rock by blasting", *Computers and Geotechnics*, 104, pp. 321–330, 2018.
<https://doi.org/10.1016/j.compgeo.2017.12.004>
- [23] Liu, K., Li, X., Hao, H., Li, X., Sha, Y., Wang, W., Liu, X. "Study on the raising technique using one blast based on the combination of long-hole presplitting and vertical crater retreat multiple-deck shots", *International Journal of Rock Mechanics and Mining Sciences*, 113, pp. 41–58, 2019.
<https://doi.org/10.1016/j.ijrmms.2018.11.012>
- [24] Hajibagherpour, A. R., Mansouri, H., Bahaaddini, M. "Numerical modeling of the fractured zones around a blasthole", *Computers and Geotechnics*, 123, 103535, 2020.
<https://doi.org/10.1016/j.compgeo.2020.103535>
- [25] Li, X., Zhu, Z., Wang, M., Wan, D., Zhou L., Liu R. "Numerical study on the behavior of blasting in deep rock masses", *Tunnelling and Underground Space Technology*, 113, 103968, 2021.
<https://doi.org/10.1016/j.tust.2021.103968>
- [26] Zhang, Z.-X., Chi, L. Y., Zhang, Q. "Effect of specimen placement on model rock blasting", *Rock Mechanics and Rock Engineering*, 54(8), pp. 3945–3960, 2021.
<https://doi.org/10.1007/s00603-021-02480-5>
- [27] Wang, Z., Zeng, Q., Lu, Z., Wan, L., Zhang, X., Gao, G. "Numerical simulation of conical pick cutting arc rock plate fracture based on ANSYS/LS-DYNA", *Advances in Materials Science and Engineering*, 2020, 6563520, 2020.
<https://doi.org/10.1155/2020/6563520>
- [28] Li, Y., Liu, C., Yu, H., Zhao, F., Wu, Z. "Numerical simulation of Ti/Al bimetal composite fabricated by explosive welding", *Metals*, 7(10), 407, 2017.
<https://doi.org/10.3390/met7100407>
- [29] Parviz, M., Aminnejad, B., Fiouz, A. "Numerical simulation of dynamic response of water in buried pipeline under explosion", *KSCE Journal of Civil Engineering*, 21(7), pp. 2798–2806, 2017.
<https://doi.org/10.1007/s12205-017-0889-y>
- [30] Li, P., Zhao, P., Lu, X. "Parameter identification and analysis of shaking table tests on SSI system", *Journal of Asian Architecture and Building Engineering*, 10(2), pp. 421–428, 2011.
<https://doi.org/10.3130/jaabe.10.421>
- [31] Zhao, Z., Wang, T., Jin, X., Zhang, L., Zhu, X., Ruan, J. "A new model of temperature-dependent permeability coefficient and simulating of pipe leakage produced immersion of loess foundation", *Bulletin of Engineering Geology and the Environment*, 82(1), 23, 2023.
<https://doi.org/10.1007/s10064-022-03043-w>